PNAS Nexus, 2022, **1**, 1–7
https://doi.org/10.1093/pnasnexus/pgac098
Advance access publication date: 5 July 2022
Research Report

Single-crystal-like germanium thin films on large-area, compliant, light-weight, flexible, single-crystal-like substrates

Kyunghoon Kim[a], Gokul Radhakrishnan[a,b], Ravi Droopad[c] and Amit Goyal[a,d,*]

[a]Tapesolar Inc., Knoxville, TN 37922, USA
[b]Now at Skorpios Technologies, Inc., Albuquerque, NM 87109, USA
[c]Ingram School of Engineering, Texas State University, 310 W Woods St 2203, San Marcos, TX 78666, USA
[d]Laboratory for Heteroepitaxial Growth of Functional Materials & Devices, Department of Chemical & Biological Engineering, State University of New York at Buffalo, 308 Furnas Hall, Buffalo, NY 14260, USA
*To whom correspondence should be addressed: Emails: goyal350@yahoo.com; agoyal@buffalo.edu
Edited By: Jainendra Jain

Abstract

Germanium (Ge) films were heteroepitaxially grown on flexible, large-area, single-crystal-like metallic substrates. Multiple, heteroepitaxial, buffer layers of nanoscale dimensions were deposited on the triaxially textured, single-crystal-like, thermo-mechanically processed Ni–W alloy substrates. Ge films were deposited on a CeO_2-terminated, heteroepitaxial buffer stack on the metallic substrate using electron beam evaporation. X-ray diffraction θ–2θ scans showed a very strong Ge (400) peak and the full width at half-maximum (FWHM) of the Ge (400) rocking curve was 0.93°. The Ge (111) ϕ-scan showed a FWHM value $\sim 4^\circ$. Based on the X-ray ω-scan, ϕ-scan and (111), (110), and (001) X-ray pole-figures, the Ge film deposited on the flexible, metallic substrate had a cube-on-cube heteroepitaxial relationship with the single-crystal-like metallic substrate. Reflection-high-energy-diffraction (RHEED) patterns from the Ge layer was streaky indicative of a smooth and essentially single-crystal-like Ge film. Cross-section TEM examination revealed a sharp interface between the Ge film and the topmost buffer layer, CeO_2, with a low defect density. The CeO_2 layer serves as a highly compliant layer that modulates its lattice parameter to attain excellent lattice-matching to the heteroepitaxial Ge layer. Ge films grown on these flexible metal substrates exhibited electron mobilities in the range of 175–250 $cm^2\ V^{-1}\ s^{-1}$. Such single-crystal-like semiconductor films on low-cost, flexible, large-area, scalable, single-crystal-like metallic substrates could potentially enable high-performance electronic devices for a range of applications.

Significance Statement:

Semiconductor-based devices are ubiquitous and have numerous potential broad-ranging applications. Besides Si, Ge-based devices of great interest. A significant barrier to realizing many of these applications relates to the limitations of the rigid semiconductor substrates for these devices that can only be made in relatively small sizes, are in-flexible and are extremely expensive. Development of alternative single-crystal substrates for Ge-based devices that are flexible, light-weight, and low-cost and upon which high-quality Ge layers can be realized could have a transformative impact on broad-ranging fields where semiconductors are used. We focus on this specific scientific and technological gap and propose a potential solution via heteroepitaxial growth of Ge layers on novel, artificial, flexible, light-weight, large-area, and low-cost substrates.

Introduction

Applications of semiconductor-based devices and systems have seen exponential growth in recent years. Use of semiconductor devices is now routine in our day-to-day living with applications in broad-ranging fields such as energy, communication, defense, consumer electronics, etc. The continuous demand to improve the performance of these devices has led to significant research in many areas to develop novel semiconductor materials as well as highly innovative device technologies that could potentially exploit these materials. However, typically these options prove expensive when implemented in large-scale manufacturing on standard semiconductor substrates. A route to significant cost-reduction, without compromising on material performance can pave way for fabrication of novel devices suitable for many electric and electronic applications. A key and significant contributor to cost in the fabrication of semiconductor devices are the materials used, especially the need to use rigid, single-crystal semiconductor substrates which can only be fabricated in limited sizes or dimensions and are extremely expensive.

An alternative prospect is to realize high-quality, heteroepitaxial single-crystal device layers on low-cost, scalable, large-area, flexible, single-crystal-like substrates. If possible, it could have a

---

Competing Interest: The authors declare no competing interests.
Received: April 12, 2022. **Accepted:** July 1, 2022

transformative impact on broad-ranging fields where semiconductors are used. In this paper, we focus on this specific scientific and technological gap and demonstrate heteroepitaxial deposition of high-quality, single-crystal-like Germanium (Ge) thin films on novel, large-area, flexible, compliant, light-weight, single-crystal-like metallic substrates.

Ge as a narrow-band-gap (1) semiconductor material has excellent crystallographic and optical properties which has led to various high-performance devices (2, 3). While it's high carrier mobility (4) has led to high speed devices (2, 3), its narrow-band-gap and high absorption coefficient have been utilized in fabricating highly sensitive optical detectors in the near infrared to visible wavelength spectrum (5–8). Also, due to the low lattice-mismatch between Ge and GaAs (0.07%), there is a huge body of research demonstrating the successful heteroepitaxial integration of III to Vs on Ge (9–12). This resulted in Ge (as template and/or as part of the active device) being used in many diverse applications such as space photovoltaic applications, terrestrial concentrated solar cells, optical sensors, high brightness LEDs, lasers, and many other applications (13).

In this work, we report on the fabrication of single-crystal-like Ge thin films on a triaxially textured, single-crystal-like, flexible metal/alloy substrates (Ni-based) fabricated via scalable, thermo-mechanical processing and with heteroepitaxially grown oxide buffer layers (14–16). The flexible, large-area, single-crystal-like substrates were fabricated by cold-rolling a metal bar in long lengths and subsequent annealing under reducing conditions to prevent oxidation. The {100} <100 > cube texture of the metal substrate has the (100) cube plane parallel to the plane of the sheet and the [100] cube edge parallel to the rolling direction. Via thermomechanical processing, a smooth surface of the metal substrate is obtained with root mean square (rms) roughness of ~50 nm. Subsequent annealing of the as-rolled, metal tape at the appropriate high temperature enables the development of a very sharp {100} <100 > cube texture and with a grain sizes in the range of 50 to 100 μm. The resulting metal substrate is an excellent starting template for the deposition of heteroepitaxial buffer layers. Compared to rigid and thick single-crystal semiconductor or oxide substrates, these substrates are significantly lighter in weight.

In order to realize the growth of semiconducting epitaxial thin films on the textured, flexible metal substrates, epitaxial buffer layers are required. The buffer layers play important roles. They enable heteroepitaxial growth and transfer of the single-crystal-like nature of the metallic substrate to the semiconductor film. They also serve as a chemical barrier to prevent deleterious elements from the metal substrate to diffuse into the semiconductor layer. In this paper, we report results on high-quality, heteroepitaxial growth of a semiconductor Ge film using electron-beam evaporation on flexible, large-area, single-crystal-like metallic substrate with a heteroepitaxial buffer layer stack of Y_2O_3, yttria-stabilized zirconia (YSZ), and CeO_2. The epitaxial Ge layer can also serve as an excellent buffer template for further heteroepitaxial of other semiconductor layers such as GaAs to realize GaAs-based semiconducting devices. Potential applications of such single-crystal, semiconductor device layers on low-cost, flexible, light-weight, large-area substrates are enormous and include a range of electronic devices including photovoltaic devices, ferroelectric devices, light-emitting diodes, magnetoresistance based devices, optoelectronics, nonvolatile memory devices, dielectric devices, thermoelectric devices, and quantum dot lasers.

Experimental

The epitaxial Ge film was grown on flexible metal substrates by e-beam deposition. Ni–5at.%W alloy tapes having a very sharp, {100} <100 > cube texture, were fabricated by cold-rolling, followed by annealing at 800~1000°C in vacuum or ambient of Ar/H_2 gas mixture for a few hours. The addition of W makes the Ni-substrate mechanically strong and less ferromagnetic. The metal tapes are flexible showing single-crystal-like orientation and with very large grain sizes (~50 to 100 μm). Heteroepitaxial buffer layers are deposited directly on top of the metallic substrate. The multilayer buffer stack consists of heteroepitaxial Y_2O_3, YSZ, and CeO_2. The important roles of the buffer films are to prevent chemical reaction with the metal tape while obtaining excellent heteroepitaxy of an oxide with a reactive metal surface (the Y_2O_3 seed layer serves this role), prevent diffusion of cations from the metal alloy substrate to the semiconductor film (the YSZ layer serves this role) and to provide an excellent lattice match for heteroepitaxial growth of the semiconductor layer (the CeO_2 layer serves this role). The top surface of the buffer stack, CeO_2 has lattice mismatch of ~4.5% with Ge film when the CeO_2 layer has a complete oxygen stoichiometry; however, oxygen stoichiometry can be modulated in CeO_2 and at a certain $CeO_{2\text{-}x}$ composition, complete lattice-matching with Ge can be obtained. All buffer layers were deposited using RF magnetron sputtering and had a thickness of ~75 nm. The growth of Ge films was performed using electron beam evaporation in vacuum (~5.0×10^{-9} torr) in the temperature range 550~700°C. Ge films had thickness thicknesses between 2 and 3 μm. The electron beam evaporation of Ge source was done using a power of 8 kV and 200~300 mA. The Ge film thickness was calculated using a quartz thickness monitor. The X-ray diffraction (XRD) of θ–2θ scan, ω and ϕ-scans were used in order to determine the thin film crystallinity, and the in-plane and out-of-plane epitaxial alignment of the deposited layer. The XRD characteristics of Ge film were evaluated using a Bede D1 diffractometer with a Cu $K_{\alpha1}$ ($\lambda = 0.15406$ nm) X-ray source. Pole-figures were generated by scanning X-ray signals with rotating the sample 360° (ϕ-scan) and tilting it from 0° to 90° (ψ-scan) at a specific θ angle in the same diffractometer. The in-situ reflection high-energy electron diffraction (RHEED) images were taken (using a 20-kV RHEED beam) from the surface of the Ge layer to monitor epitaxial film growth. The interface of Ge and the buffer film was examined using cross-section transmission electron microscopy (TEM). The sample was prepared using a focused-ion beam (FIB) method and imaging was done using JEOL 2010 TEM system. The electronic properties of Ge layers were characterized via Hall measurements using a Bio-Rad Accent HL5500 Hall system with a magnetic field of 0.325 T. Carrier mobility, bulk carrier concentration, and resistivity were measured using this system and all measurements were done at room temperature on a square geometry with four indium ohmic contacts placed at the edges of the 10 mm square samples. A current of 0.1 mA was used during the measurement and the results (mobility and carrier concentration) were displayed on the screen.

Results and discussion

Fig. 1 shows a schematic diagram of the Ge layer and heteroepitaxial buffer stack on the flexible metal substrate. Images on the right show the RHEED patterns that were taken from the surface of (a) CeO_2 before Ge deposition and (b) 2D Ge layer deposited on top layer CeO_2 buffered metal substrate, grown under optimized growth conditions.

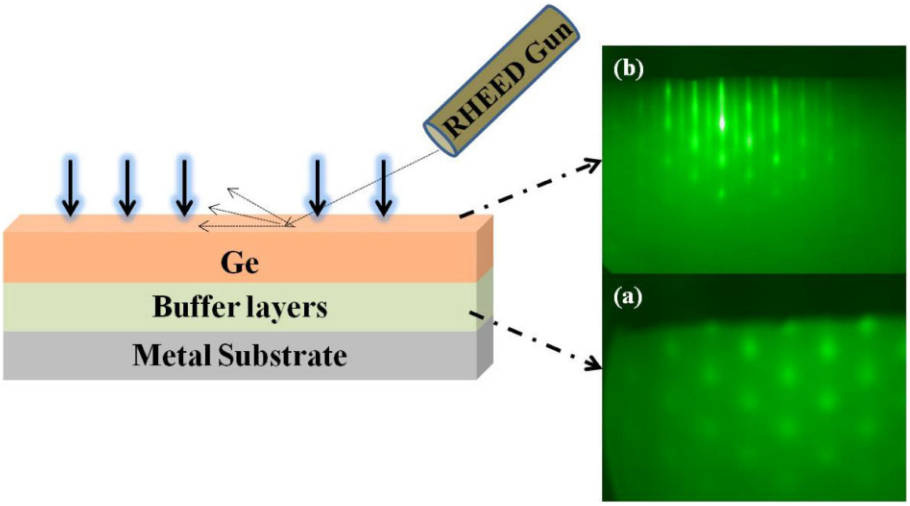

Fig. 1. Schematic of Ge layer deposited on the buffer stack and metal substrate (left) and the in-situ RHEED pattern (right) of (a) CeO_2 film prior to start of deposition (b) smooth streaky 2D Ge film deposited on buffer stack and metal substrate.

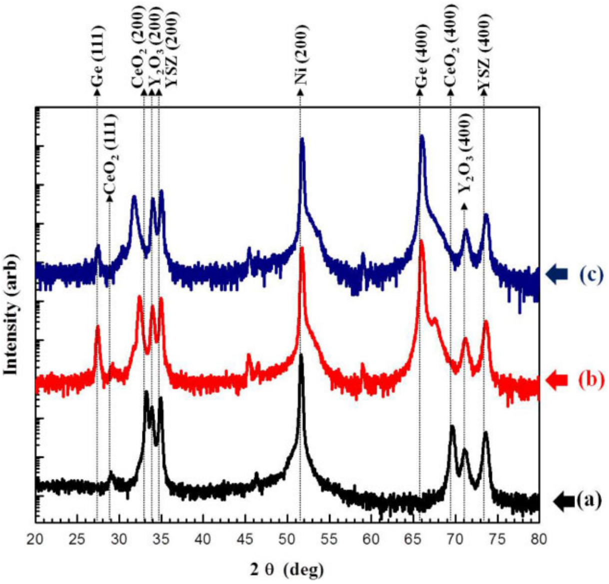

Fig. 2. The X-ray diffraction θ–2θ scan graphs of (a) single-crystal-like metallic substrate including buffer stack. (b) Ge film grown on buffer stack and metal substrate at low temperature. (c) Ge film grown on buffer stack and metal substrate at high temperature.

The buffer layers and metal substrate are aligned to within a few degrees with respect all three crystallographic axis at all points in the large-area substrate having a single-crystal-like orientation and having very large grain sizes. Fig. 2a shows the X-ray diffraction θ–2θ scan of the single-crystal-like, Ni–W metallic alloy substrate with heteroepitaxial oxide buffer layers of Y_2O_3, YSZ, and CeO_2. Ni-W XRD (200) peak appears at 51.6°.

The peaks representing CeO_2 (200) and CeO_2 (400) reflections appear at 33.0° and 69.5°, respectively. XRD peaks of Y_2O_3 (200) and Y_2O_3 (400) appear at 33.9° and 71.1°, respectively. XRD pattern of YSZ (200) and YSZ (400) appear at 34.9° and 73.6°, respectively. Fig. 2a indicates that the CeO_2 terminated buffer layers were grown having a (00*l*) orientation on top of the Ni–W metal substrate. Several growth recipes were explored to obtain the ideal deposition conditions for high quality epitaxial growth of Ge on CeO_2 terminated buffer layers. The Ge layer was deposited at varying nucleation temperatures ranging from 500°C to 750°C and at a deposition rate ranging from 0.2 to 1 μm/h. By using in-situ RHEED analysis of the surface quality and XRD analysis of the crystal quality, it is clear that higher nucleation temperature leads to improved quality of the epitaxial Ge layer.

Fig. 2b shows the θ–2θ scan graph of Ge film deposited on the (00*l*) oriented buffer stack and metal substrate. This Ge film was nucleated at 600°C using electron beam evaporation on the (00*l*) oriented cerium oxide, which is the top layer of the buffer stack on the metal substrate. The Y-axis which indicates the intensity is shown on a logarithmic scale to separate the peaks clearly. From the X-ray θ–2θ scan, a strong and dominant Ge (400) peak can be observed at around 66.0°. The (00*l*) oriented buffer stack and metal substrate peaks are also shown in the X-ray scan. The minor peaks at 27.6° and 45.6° are from Ge (111) and (220) orientation. According to the X-ray θ–2θ scan, Ge film with (400) orientation was obtained on the cerium oxide terminated metal substrate. The CeO_2 (200), (400) peaks at 33.0°, 69.5° in Fig. 2a were observed to be shifted to the left after Ge film deposition which could be clearly seen at Fig. 2b. The lattice mismatch between Ge and CeO_2 (Ge: 5.658 Å, CeO_2 : 5.410 Å) can be calculated to be 4.6%. During Ge film deposition at the elevated temperature of >600°C under a reducing environment, volume expansion of CeO_2 occurs due to increased oxygen deficiency within the CeO_2 layer. As a result, the (00l) CeO_2 peaks are shifted to the left from their original positions for stochiometric CeO_2.

The shifted (400) CeO_2 peak is closer to the (400) Ge peak. However, CeO_2 peaks at 27.6° and 45.6° from Ge (111) and (220) orientation indicate some polycrystalline components. Fig. 2c is the θ–2θ scan graph of the Ge film deposited at 750°C on the (00*l*) oriented cerium oxide top buffer layer on the metal substrate. There is a clear and larger left shift of the (00*l*) CeO_2 peaks. The shifted (400) CeO_2 peak has now merged with the (400) Ge peak. This indicates that the Ge film is now essentially *lattice-matched* with the CeO_2 terminated buffer stack indicating the highly compliant nature of the CeO_2 layer resulting in excellent lattice-matching of $CeO_{2\text{-x}}$ with Ge. This peak shift enables realization of heteroepitaxial film growth with few defects in the Ge layer due to lattice-matching. A closer look at the X-ray diffraction scans is shown in Fig. 3 and the merging

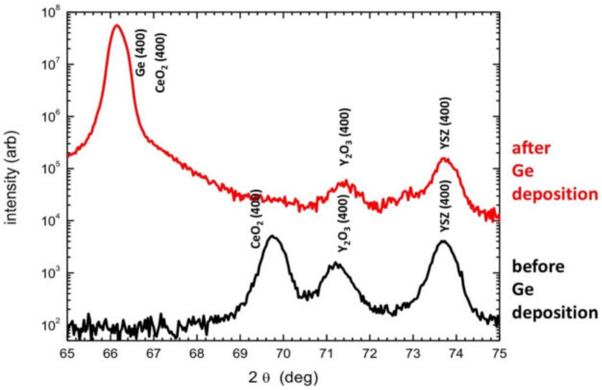

Fig. 3. Zoomed-in X-ray diffraction θ–2θ scans of top buffer layer, CeO_2, and the Ge film. As can be clearly seen, the CeO_2 (400) peak is now merged with the Ge (400) peak after deposition under highly reducing conditions.

of the (400) CeO_2 peak with the (400) Ge peak can be clearly seen. Also, there is significant reduction in the peaks at 27.6° and 45.6° from Ge (111) and (220) orientations. The RHEED pattern of Fig. 1b was taken from the surface of the Ge layer nucleated at 750°C. The nice streaky pattern indicates that the Ge film surface is smooth and heteroepitaxial on the buffer stack and metal substrate.

The X-ray diffraction scans in Fig. 4 shows the orientation of the out-of-plane alignment when rocking in the rolling direction for both (a) (400) Ge and (b) (200) CeO_2 reflections. The full width at half-maximum (FWHM) value of the Ge film rocking curve is 0.93° demonstrating that all the grains in Ge film are aligned to within 1°. The X-ray diffraction rocking curves taken from the perpendicular direction is shown in Fig. 4 for both (c) (400) Ge and (d) (200) CeO_2. The FWHM values of the (400) Ge in both the rolling and perpendicular directions indicate that the Ge film is epitaxially deposited on CeO_2 terminated buffer stack of metal substrate with excellent out-of-plane orientation. FWHM values of the rocking curve are the result of the slight differences in orientation between the large individual Ge grains with the average grain size of 50 to 100 μm.

The XRD ϕ-scans in Fig. 5 show the in-plane texture or orientation of (a) (111) Ge and (b) (111) CeO_2 reflections and suggest that all the grains in the Ge layer are aligned in-plane to within 4°. Fig. 5 indicates that a cube-on-cube heteroepitaxial relationship was observed for the Ge film on CeO_2 terminated buffer stack on metal substrate. Such a Ge surface is single-crystal-like with a grain size of about 100 microns. Within a single grain, the Ge is essentially single-crystal.

Fig. 6 shows the X-ray pole-figures of (a) (100) Ge, (b) (110) Ge, and (c) (111) Ge. The four-fold symmetric poles indicate that the Ge film is both in-plane and out-of-plane aligned. This pole-figure covers 100s of large grains of Ge which are all fully-aligned. In addition to this, the volume fraction of the cube-texture is ~100%. Such a Ge film could potentially be extremely useful for broad-ranging electronic applications or for use as a flexible Ge substrate for growth of other device layers such as GaAs.

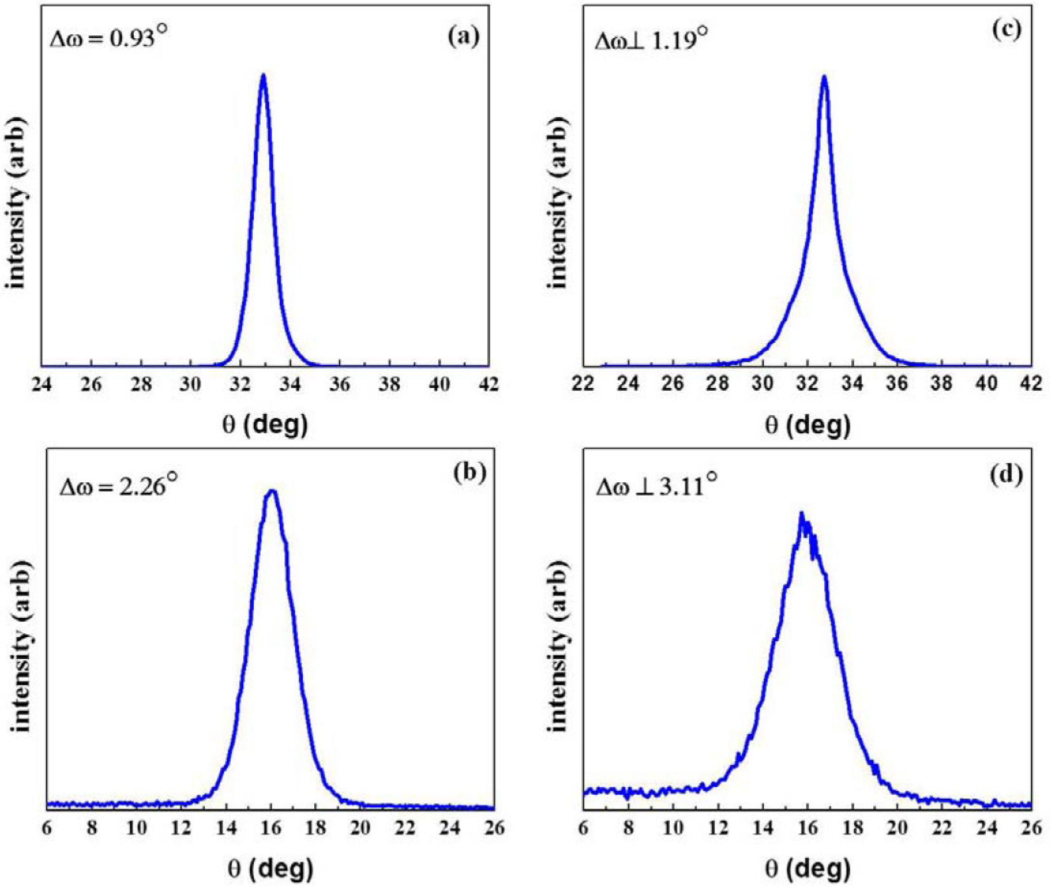

Fig. 4. The X-ray diffraction ω-scans of (a) Ge (400) and (b) CeO_2 (200) planes in the rolling direction and X-ray diffraction ω-scans of (c) Ge (400) and (d) CeO_2 (200) planes in the perpendicular direction. The intensity is plotted on a linear scale in arbitrary units.

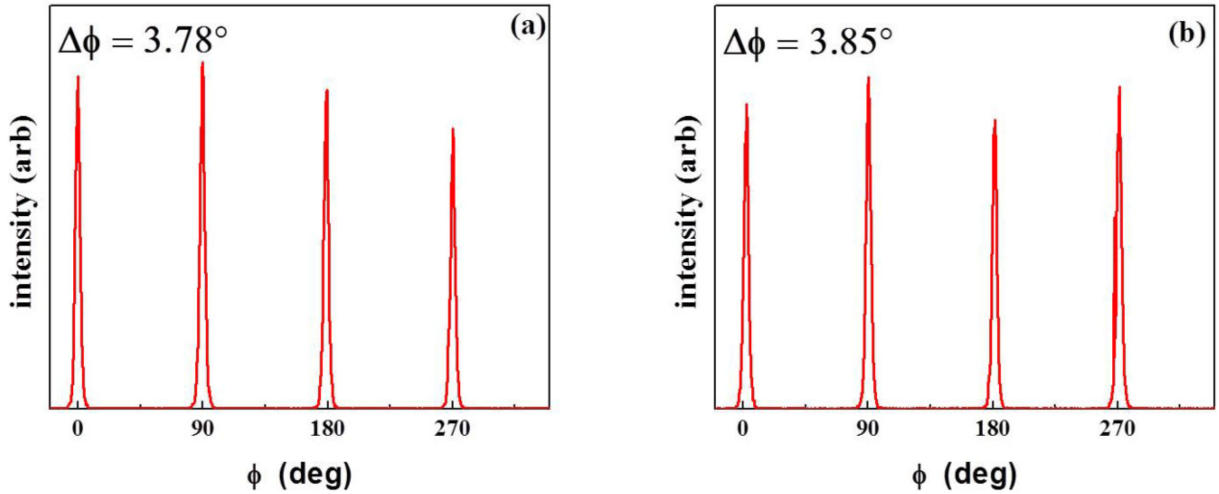

Fig. 5. The X-ray diffraction ϕ-scans of (a) Ge (111) and (b) CeO$_2$ (111) planes. The intensity is plotted on a linear scale in arbitrary units.

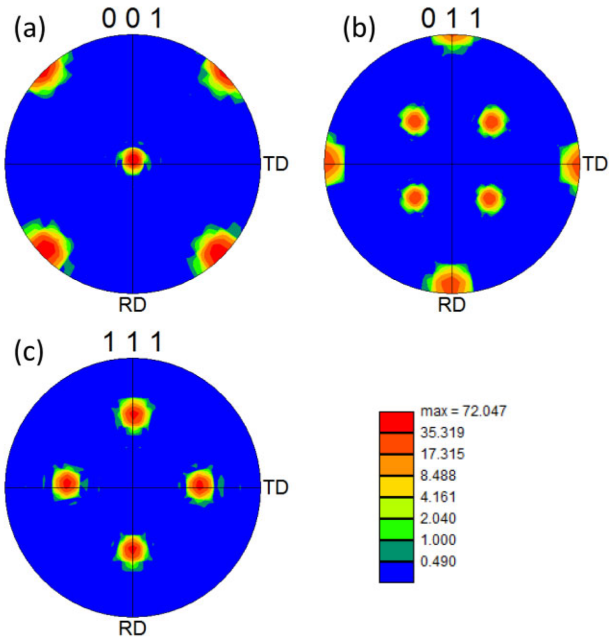

Fig. 6. The X-ray pole-figures of (a) (001) Ge, (b) (011) Ge, and (c) (111) Ge.

Detailed cross-section TEM examination was carried out on the Ge film deposited on the CeO$_2$ terminated buffer stack. Fig. 7 shows TEM images of the interface between the Ge film and CeO$_2$ layer. Fig. 7a shows a low-magnification image of the sample cross-section of the Ni–W substrate/Y$_2$O$_3$/YSZ/CeO$_2$/Ge stack. Fig. 7b shows a higher-magnification image of the YSZ/CeO$_2$/Ge interfaces. Some of the diffraction contrast in the CeO$_2$ layer may be arising from regions of oxygen deficiency. Fig. 7c shows a higher-magnification image of the CeO$_2$/Ge interface. A sharp interface is observed between Ge film and the CeO$_2$ buffer cap layer. The continuous lattice fringes of Ge film and CeO$_2$ buffer layer can also be observed which indicates that the Ge film has good heteroepitaxy. The top buffer layer, CeO$_2$, is essentially lattice-matched to Ge as explained previously using X-ray θ–2θ scans. Fig 7d shows a selected area diffraction patterm from the Ge layer indicating the single-crystal nature of the Ge film.

Fig. 8 is the TEM image the Ge film. Fig. 8a shows that several antiphase boundaries labeled as T1 and T2 can be observed near the CeO$_2$/Ge interface which self-annihilate themselves at a thickness less than 100 nm within the Ge layer. Beyond this thickness, there are only a few dislocations and essentially a defect free region in the Ge layer as shown in Fig. 8b.

In order to explore the electronic properties of the Ge layer, hall measurements were performed. An *n*-type Ge layer of 3 μm thickness was deposited on CeO$_2$ buffer layer to measure mobilities. The insulating CeO$_2$ layer along with the other buffer oxide layers act as an effective barrier for performing Hall measurements. Under ideal growth conditions, the Ge layers showed excellent carrier mobility. Electron mobilities in the range of 175 to 250 cm^2 V^{-1} s^{-1} were obtained for Ge layers heteroepitaxially deposited on the metallic substrate with *n*-type bulk carrier concentration of 4 × 10^{18} cm^{-3}. This is very high mobility compared to that for polycrystalline, nonsingle-crystal-like semiconductor layers and compares well with mobilities obtained for single crystal Ge films with similar doping densities.

Conclusions

Ge films were heteroepitaxially grown on flexible, large-area, light-weight, single-crystal-like metallic substrates using electron beam evaporation in vacuum in the temperature range of 600∼700°C with a thickness of 2 to 3 μm. Several heteroepitaxial, oxide buffer layers of nanoscale dimensions were grown on the Ni–W substrate and terminated with a CeO$_2$ layer which makes for a highly compliant layer for lattice-matching with the Ge layer. The X-ray θ–2θ scans indicated lattice-matching of Ge with the modified CeO$_{2\text{-x}}$ layer. X-ray ω-scans and ϕ-scans showed sharp in-plane and out-of-plane alignment of the heteroepitaxial Ge film on CeO$_{2\text{-x}}$ terminated buffer stack of the metal substrate. Cross-section TEM images indicated a sharp interface between the Ge film and CeO$_{2\text{-x}}$ buffer layer as well as termination of antiphase boundaries within a 1-μm layer from the CeO$_2$/Ge interface. A *n*-type Ge layer deposited on CeO$_2$ buffer layer showed electron mobilities in the range of 175 to 250 cm^2 V^{-1} s^{-1}. The Ge film is essentially single-crystal-like with a very low defect density. Such high-quality, heteroepitaxial Ge layers deposited on the flexible, compliant, large-area, light-weight, single-crystal-like metal substrate can potentially be used for fabricating a range of electronic

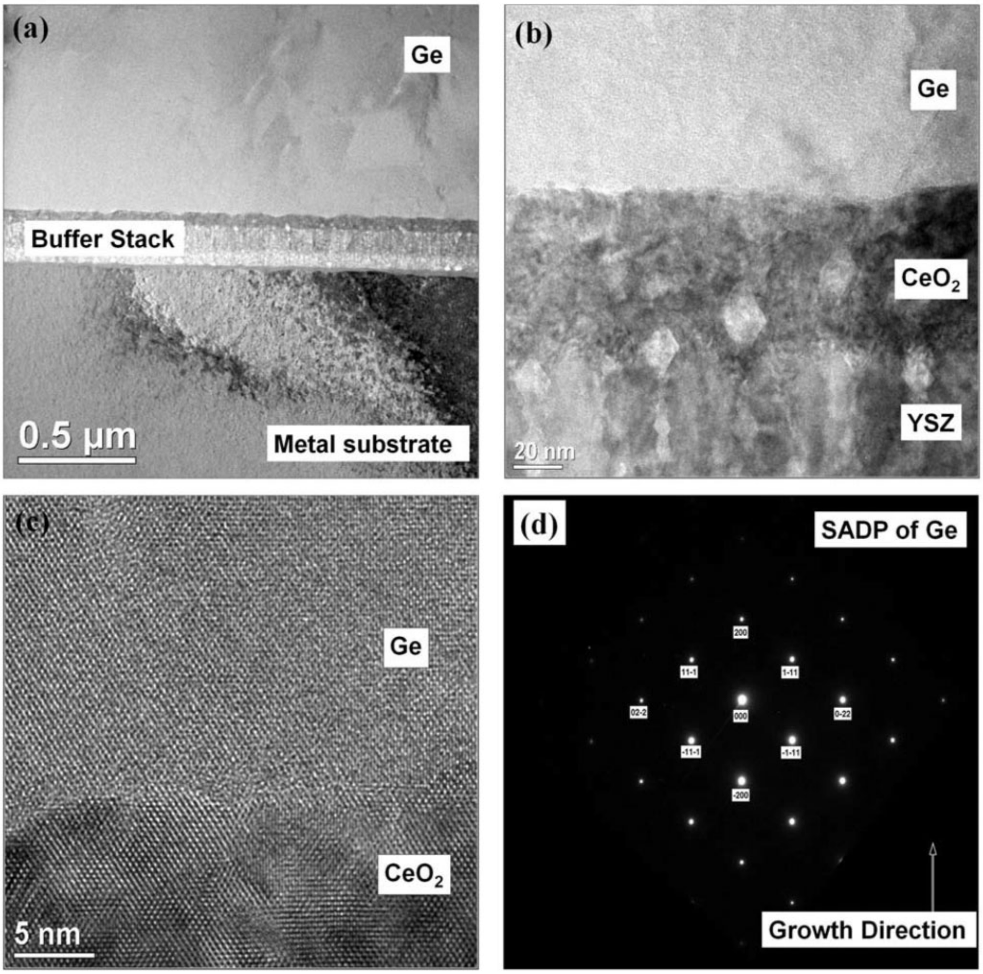

Fig. 7. Cross-section TEM images of Ge film grown on CeO_2 terminated buffer stack of metal substrate. (a) Low-magnification image of the sample cross-section of the Ni–W substrate/Y2O3/YSZ/CeO2/Ge stack; (b) Higher-magnification image of the YSZ/CeO2/Ge interfaces; (c) Cross-section TEM image of CeO2/Ge showing good heteroepitaxial growth; (d) Selected area diffraction pattern from the Ge layer indicating the single-crystal nature of the Ge film.

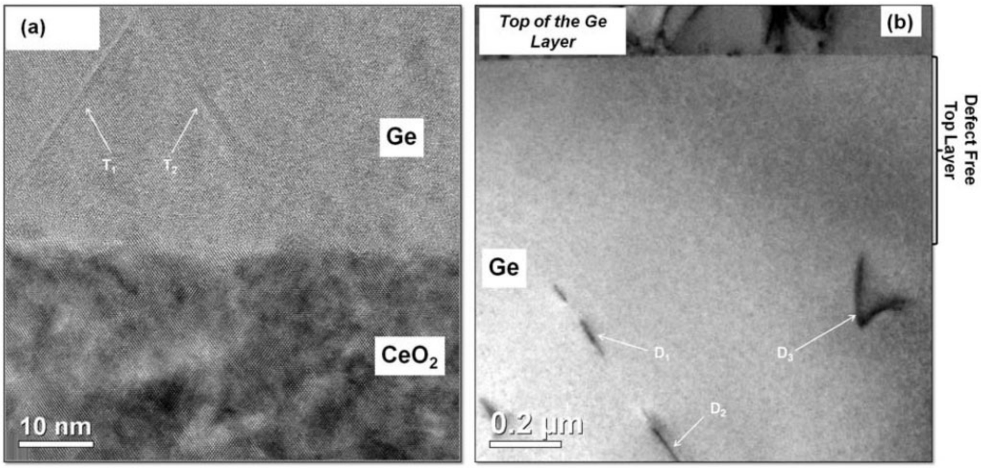

Fig. 8. Cross-section transmission electron microscopy (TEM) image of Ge film grown on CeO_2 terminated buffer stack of metal substrate: (a) near the CeO2/Ge interface; (b) At the top of the Ge film.

devices or as a flexible semiconductor substrate for growth of additional semiconductor layers.

Funding

The authors declare no funding.

Authors' Contributions

K.K. preformed the research, analyzed data, and wrote the paper; G.R. contributed to the experiments and analysis of data; R.D. contributed to tools and facilities used for the work, and to the analysis of the data; A.G. designed and supervized the research, contributed to analysis of data, and writing of the paper.

Data availability

All data is included in the manuscript.

References

1. Collings PJ. 1980. Simple measurement of the band gap in silicon and germanium. Am J Phys 48:197.
2. Patton GL, *et al.* 1990. High electron mobility in modulation-doped Si/SiGe. Electron Device Lett 11:171.
3. Goley PS, Hudait MK. 2014. Germanium based field-effect transistors: challenges and opportunities. Materials 7:2301.
4. Prince MB. 1953. Drift mobilities in semiconductors. I. Germanium. Phys Rev 92:681.
5. Fama S, Colace L, Masini G, Assanto G, Luan HC. 2002. High performance germanium-on-silicon detectors for optical communications.Appl Phys Lett 81:586.
6. Dehlinger G, *et al.* 2004. High-speed germanium-on-SOI lateral PIN photodiodes. IEEE Photonics Technol Lett 16:2547.
7. Chen L, Lipson M. 2009. Ultra-low capacitance and high speed germanium photodetectors on silicon. Opt Express 17: 7901.
8. Michel J, Liu J, Kimerling L. 2010. High-performance Ge-on-Si photodetectors. Nature Photon 4:527–534.
9. King RR, *et al.* 2007. 40% efficient metamorphic GaInP/GaInAs/Ge multijunction solar cells. Appl Phys Lett 90:183516.
10. Gutera W, *et al.* 2009. Current-matched triple-junction solar cell reaching 41.1% conversion efficiency under concentrated sunlight. Appl Phys Lett 94:223504.
11. Modak P, *et al.* 2000. (AI)GaInP multiquantum well LEDs on GaAs and Ge. J Elect Mat 29:80–85.
12. Marris-Morini D, *et al.* 2018. Germanium-based integrated photonics from near- to mid-infrared applications. Nanophotonics 7:1781–1793.
13. Bosi M, Attolini G. 2010. Germanium: epitaxy and its applications. Prog Cryst Growth and Charact Mater 56: 146–174.
14. "Semiconductor-based, large-area, flexible, electronic devices. Amit Goyal, US Patent 7,906,229, March 15, 2011.
15. "{100}<100>or 45°-Rotated {100}<100>, Semiconductor-Based, Large-Area, Flexible, Electronic Devices," Amit Goyal, US Patent US 8,178,221 B2, May 15, 2012.
16. "[100]or [110]aligned, semiconductor-based, large-area, flexible, electronic devices. Amit Goyal, US Patent 8,987,736, March 24, 2015.